EVALUATION OF DAMAGE IN DIFFERENT CONCRETES: FRACTAL ANALYSIS AND RELATION TO TOUGHNESS CHARACTERISTICS

B. Chiaia*† and J.G.M. Van Mier*

The fractality of fracture patterns induced by splitting tests is investigated for four concrete. Image processing techniques are used to extract the crack topology from digitized images. The Box-Counting method is applied to the crack networks to measure their fractal properties. The fractal analysis can successfully describe the progressive vanishing of microstructural disorder effects, related to different scales of observation of the process. No clear correlation was found between the fractal dimension and the fracture energy in the composites. The most relevant effect of the invasive fractality of damage is the crack-resistance behaviour encountered in the tests.

INTRODUCTION: FAILURE IN DIFFERENT TYPES OF CONCRETE

Deformation-controlled splitting tests on notched concrete specimens have been carried out. Details of the test set-up are described by Vervuurt et al. (1). Four different mixtures have been tested. Two mixtures were casted using traditional river gravel, with maximum aggregate size of 16mm (Con16) or 2mm (Con2). A third mixture was made containing phosphorous-slag aggregates (ConPS). Finally, a porous lightweight aggregate was used (Lytag) in the fourth mix. A minimum number of three specimens was tested for each batch of concrete. From Table 1, it can be seen that ConPS shows the highest peak load, whereas Con16 is characterized by the highest fracture energy. The largest work of fracture, computed up to 100μm displacement, is measured for ConPS. On the other hand, if the ratio between fracture energy and tensile strength is taken as a measure of ductility, Con16 seems more favourable, whereas phosphorous-slag concrete is the most brittle material. In fact, ConPS is characterized by pronounced local instabilities, probably due to the high stiffness of the phosphorous aggregate which yields to rather brittle interface debonding.

* Dept. of Civil Engineering, Stevin Laboratories, Delft University of Technology
† Dept. of Structural Engineering, Politecnico di Torino

The relative brittleness of the lightweight concrete is usually explained from the weakness of the Lytag particles, which lowers the crack-arresting capacity. Indeed, Lytag particles are heterogeneous at the micro-level. The fractal dimension of the cracks *through* these particles is considerably high when compared to the fractal dimension of the whole composite. This may explain the stable crack growth occurring in the Lytag, which is not trivial compared to its low global toughness.

Next to the lower mechanical performances, the Lytag and the Con2 are characterized by a much lower scatter of the measured mechanical properties, when compared to Con16 and ConPS. This can be explained by the *lower degree of microstructural disorder* at the specimen level. In fact, the lightweight concrete is characterized by uniform mechanical properties for both the matrix and the particles. The Con2 is a finer-grained mixture. As it will be explained furtheron, a more rapidly vanishing fractality occurs in these materials.

TABLE 1 - Results from the Splitting Tests on the four Concrete Mixtures.

Concrete type		Max load P_u (N)	Max displ. δ (μm)	Work of fracture ($\delta < \delta_{max}$) (N×m)	Work of fracture ($\delta < 100$) (N×m)	Fracture energy ($\delta < \delta_{max}$) (N/m)	Fracture energy ($\delta < 100$) (N/m)
Con16	mean	509.68	134.1	0.04338	0.03744	40.35	36.05
	stdev	43.17	50.02	0.01883	0.00849	25.07	13.65
Con2	mean	489.98	166.7	0.04696	0.03547	36.63	27.78
	stdev	29.50	3.96	0.01295	0.00763	10.45	7.02
Lytag	mean	430.62	116.2	0.03500	0.03156	24.89	22.10
	stdev	41.25	33.54	0.00746	0.00251	5.68	2.98
ConPS	mean	562.19	129.1	0.04617	0.04435	31.40	30.89
	stdev	52.63	53.36	0.01891	0.00413	16.95	10.01

IMAGE PROCESSING AND BOX-COUNTING ANALYSIS

In addition to the classical mechanical measurements, optical detection of the propagating cracks has been performed in a small region around the notch tip. The automatic scanning of the specimen surface during the loading process has been carried out by means of the computer-controlled QUESTAR Remote Measurement System described in (1). After breaking of the specimen, mosaics are created by the computer by linking the single images belonging to a prescribed crack path. The obtained mosaic, results in a lower resolution with respect to the original images. They represent a global view of the damage, and can be adopted to describe the

transition from the fractal patterns detected at the highest magnifications to the euclidean domains usually observed when the scale of observation decreases.

In order to extract the topological information about the damage patterns, filtering of the images is necessary. Starting from complex gray-level images, pixels belonging to the cracks have to be selected and isolated. Thresholding does not turn into a straightforward procedure because discrimination between cracks and dark particles is extremely difficult. Therefore, prior to thresholding, the contrast in the image was enhanced by eliminating a sufficient number of graylevels. Afterwards, selective thresholding has been applied to different parts of the image, choosing for each zone the most appropriate threshold value. Minor corrections were sometimes necessary to eliminate isolated black pixels.

After thresholding, binary thinning of the cracks was applied in two different ways. The first algorithm yielded skeletonized cracks by averaging black pixels through the width. A serious drawback was the loss of many details from the crack boundaries, resulting in smoother thinned patterns not properly representing the complexity of the energy dissipation which takes place at the crack lips. It was decided to develop a second algorithm which was capable to outline the cracks by isolating their boundaries. Afterwards, the Box-Counting method can be applied to the crack networks (Fig. 1). As the size ε of the boxes decreases, their number N increases and the area of the cover E decreases. The *Box-dimension* Δ is obtained:

$$\Delta = \lim_{\varepsilon_i \to 0} \left(\frac{\log N(\varepsilon_i)}{\log (1/\varepsilon_i)} \right) = 2 - \lim_{\varepsilon_i \to 0} \left(\frac{\log |E(\varepsilon_i)|_2}{\log \varepsilon_i} \right). \qquad (1)$$

Linear regression is carried out in the log$N$ vs. logε plot or in the log$E$ vs. logε plot. The slopes φ and ϑ are respectively obtained. From these values, the Box-dimension Δ is yielded as $\Delta=-\varphi$ or as $\Delta=2-\vartheta$. Further details of the algorithm are described by Mandelbrot (2).

Rigorously speaking, the isotropic shrinking of the covering grids implies self-similar scaling of the covering shape. This could be in contrast with the eventually anisotropic (self-affine or multifractal) properties of the fractal domain. Looking at the experimental cracks from farther, self-affine aspects increase (2). Therefore, direction-dependent rescaling of the grid should be performed. This relatively awkward procedure can be avoided if anisotropic grids are used, for example by means of rectangular boxes, to enhance the statistical fluctuations in one direction. In this way, it is possible to detect the local fractal dimension in the limit of the smallest grids. In case of the high-resolution images the orthotropy directions continuously change. In addition, crack branching and secondary cracks can be detected. Therefore, it seemed more convenient to use isotropic square coverings of the high-resolution patterns, since damage at that scale possesses self-similar character.

FRACTAL CHARACTERISTICS OF THE DIGITIZED CRACK PATTERNS

The optical detection of the damage permits to highlight some morphological differences in the fracture behaviour of the different concretes, which correspond to the previously described mechanical differences. The interface between large aggregates and matrix represents the weakest link of the four composites. In the case of the ConPS, the propagation of the cracks is almost totally controlled by the bond strength, and the irregular shape of the aggregates contributes to an increase of the toughness characteristics. On the other hand, when the aggregate strength is comparable to the strength of the matrix, interface failure plays a less important role. A lead role is played by the porosity of the particles, which enhances the bonding strength as in the case of Lytag (3).

In the case of Lytag and Con2, a more homogeneous behaviour (at the global level) has been detected. Cracks propagate through the particles in the Lytag and the fracture patterns in Con2 are relatively smooth. On the other hand, microscopic bridging is activated at the scale of sand grains in the Con2, as well as rough fractal cracks grow through the Lytag particles. This means that disorder is equally present in those two materials, but at *a lower level*, compared to Con16 and ConPS.

TABLE 2 - Measured Fractal Dimensions.

Image →	High resol. (0.71 pix/μm)		Standard res. (0.278 pix/μm)		Mosaics high res.		Mosaics standard res.	
Concrete ↓	min-max Δ	mean Δ	min-max Δ	mean Δ	min-max Δ	mean Δ	min-max Δ	mean Δ
Con16	1.16÷1.33	1.25	1.09÷1.22	1.14	1.05÷1.20	1.13	1.06÷1.13	1.08
Con2	1.08÷1.30	1.18	1.07÷1.19	1.10	1.05÷1.16	1.10	1.02÷1.04	1.03
Lytag	1.13÷1.35	1.24	1.05÷1.20	1.10	1.04÷1.15	1.09	1.03÷1.08	1.04
ConPS	1.14÷1.29	1.18	1.08÷1.20	1.14	1.07÷1.18	1.13	1.05÷1.14	1.07

Non-integer topological dimensions of the damage patterns have been found by means of the Box-Counting method in the four concretes. This confirms that, at the proper scales, the phenomenon of fracture in concrete possesses a well-defined fractal character. A general trend has been revealed for the four different concretes: as the resolution of the image decreases, the fractal dimension decreases as well (Fig. 2). A transition from fractal topologies at small scales towards homogeneous patterns at larger scales (*geometrical multifractality*) occurs in all the four mixtures. Multifractality implies the progressive homogeneization of the microstructural fluctuations, which is reflected by progressive vanishing of the scaling properties of disordered materials for increasing structural size (Carpinteri and Chiaia (4)).

Boundary thinning was preferred in presence of self-affine patterns, since in this way it was possible to enhance the crack lip's irregular fluctuations orthogonally to the advancement direction. Thereby, the local fractal dimension was calculated. If the mean values of the fractal dimension Δ of the different concretes are compared (Table 2), it can be stated that homogeneization of the disordered microstructure is observed earlier for the case of Lytag and Con2. Therefore these mixtures are characterized by a smaller internal length. This may explain the lower scatter in the measurement of their mechanical properties

CONCLUSIONS

The stiffness, strength and density of the aggregates strongly affect the behaviour of concrete. The vitreous consistency of the phosphorous-slag accounts for the high strength and hardeness of the ConPS mixture. Pronounced local instabilities occur during the fracture process. These correspond to sudden debonding of the interface between matrix and aggregate. A more brittle structural behaviour is therefore provided by this type of concrete, when compared to the normal or Lytag mixtures. The weakness of the Lytag particles yields a reduced crack-arresting capacity in the lightweight concrete. A stronger bond between the matrix and the particle results in a more homogeneous damage propagation. On the other hand, fractal cracks often develop through the particles, and local instabilities (snap-backs) are almost absent. This may be the reason for the relevant structural ductility found on this type of composite, which is not obvious if related to its low toughness and strength. Moreover, a reduced sensitivity to thermic and shrinkage cracks is present, due to the similar elastic modulus possessed by the matrix and the Lytag aggregates.

Higher fractal dimensions do not imply higher fracture energy in a material, because disordered fracture patterns may be the consequence of both weak (pores, bonds) and strong (aggregates, inclusions) heterogeneities. No correlation is found between the fractal dimensions and the measured fracture energy. Instead, fractality permits to explain the *stable crack growth* occurring in the first stages of loading. Whilst, in the case of smooth cracks, the *crack-resistance* is independent of crack length a, in the presence of fractal cracks it increases with a, following a power-law with exponent equal to the fractal dimensional increment $d_{\mathcal{G}}$ ($d_{\mathcal{G}} = \Delta - 1$) of the fracture domain (3). Moreover, since the *global* fractal increment $d_{\mathcal{G}}$ progressively tends to zero as the damage spreads, a *plateau* in the R-curve is always detected.

REFERENCES

(1) Vervuurt, A., Chiaia, B. and Van Mier, J.G.M., Heron, Vol. 40, No. 4, 1996.
(2) Mandelbrot, B.B., "The Fractal Geometry of Nature." W.H. Freemann & Company, New York, USA, (1982).
(3) Zhang, M.H. and Gjorv, O.E., Cem. & Con. Res., Vol. 20, 1990.
(4) Carpinteri, A. and Chiaia, B., Mater. & Struct., Vol. 28, 1995, pp. 435-443.

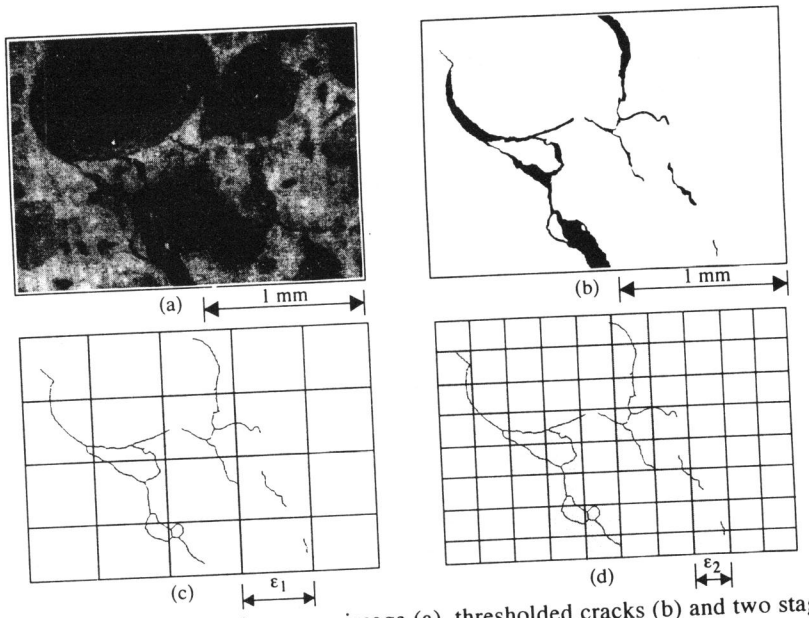

Figure 1. Gray-level microscope image (a), thresholded cracks (b) and two stages of the Box-Counting analysis on the thinned damage patterns (c, d).

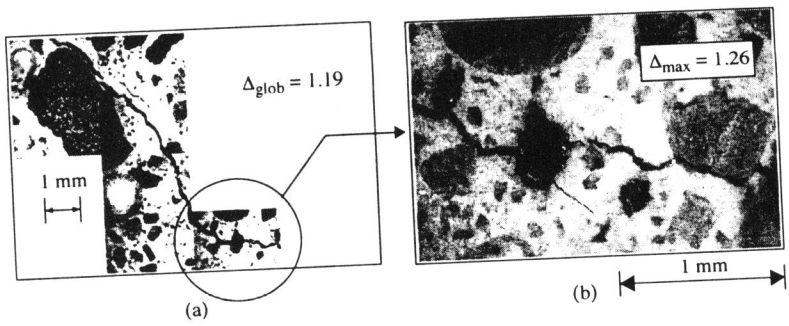

Figure 2. Damage at various scales in Con16: low-resolution mosaic (a) and high resolution image (b).